View Journal

Dalton Transactions

Accepted Manuscript

This article can be cited before page numbers have been issued, to do this please use: A. Foi, F. D. Salvo, F. Doctorovich, C. Huck-Iriart, J. Ramallo-Lopez, M. Dürr, I. Ivanovi-Burmazovi, K. Stirnat, S. Garbe and A. Klein, *Dalton Trans.*, 2018, DOI: 10.1039/C8DT02549E.

This is an Accepted Manuscript, which has been through the Royal Society of Chemistry peer review process and has been accepted for publication.

Accepted Manuscripts are published online shortly after acceptance, before technical editing, formatting and proof reading. Using this free service, authors can make their results available to the community, in citable form, before we publish the edited article. We will replace this Accepted Manuscript with the edited and formatted Advance Article as soon as it is available.

You can find more information about Accepted Manuscripts in the author guidelines.

Please note that technical editing may introduce minor changes to the text and/or graphics, which may alter content. The journal's standard Terms & Conditions and the ethical guidelines, outlined in our author and reviewer resource centre, still apply. In no event shall the Royal Society of Chemistry be held responsible for any errors or omissions in this Accepted Manuscript or any consequences arising from the use of any information it contains.

ROYAL SOCIETY OF CHEMISTRY

rsc.li/dalton

View Article Online
DOI: 10.1039/C8DT02549E

Synthesis and Structural Characterisation of Unprecedented Primary *N*-nitrosamines Coordinated to Iridium(IV)†

Ana Foi,[a] Florencia Di Salvo,*,[a] Fabio Doctorovich,*,[a] Cristián Huck-Iriart,[bc] José Martín Ramallo-López,[b] Maximilian Dürr,[d] Ivana Ivanović-Burmazović,[d] Kathrin Stirnat,[e] Simon Garbe[e] and Axel Klein*,[e]

[a] Departamento de Química Inorgánica, Analítica, y Química Física, Facultad de Ciencias Exactas y Naturales, Universidad de Buenos Aires, INQUIMAE-CONICET, Ciudad Universitaria, Pabellón 2, Piso 3, C1428EHA Buenos Aires, Argentina; E-mail: flor@qi.fcen.uba.ar; doctorovich@qi.fcen.uba.ar

[b] Instituto de Investigaciones Fisicoquímicas Teóricas y Aplicadas (INIFTA), Facultad de Ciencias Exactas, Universidad Nacional de La Plata, CONICET, Casilla de Correo 16, Sucursal 4, 1900 La Plata, Argentina.

[c] Escuela de Ciencia y Tecnología, CONICET, Universidad Nacional de San Martín (UNSAM), Campus Miguelete, 25 de Mayo y Francia, 1650 San Martín, Provincia de Buenos Aires, Argentina

[d] Lehrstuhl für Bioanorganische Chemie, Friedrich-Alexander-Universität Erlangen-Nürnberg, Egerlandstr. 1, 91058 Erlangen, Germany

[e] University of Cologne, Department of Chemistry, Institute for Inorganic Chemistry, Greinstrasse 6, D-50939 Cologne, Germany; E-Mail: axel.klein@uni-koeln.de

ORCID: Axel Klein: 0000-0003-0093-9619; Florencia Di Salvo: 0000-0001-7295-2471; Fabio Doctorovich: 0000-0003-1088-2089

Received: Dalton Transactions

†Electronic supplementary information (ESI) available: A table with detailed UV-vis spectroelectrochemical data and thirteen figures showing NMR spectra monitoring oxidation and decomposition reactions as well as UV-vis absorption, NMR and XANES spectra of (PPh_4)**[1]** are provided. See DOI: 10.1039/xxx

Keywords: primary *N*-nitrosamines • iridium • electrochemistry • spectroelectrochemistry • Ir L_3 XANES

Abstract

View Article Online
DOI: 10.1039/C8DT02549E

The redox chemistry of the *N*-nitrosamine complexes $[IrCl_5(RN(H)N=O)]^{2-}$ (R = benzyl or *n*-butyl) was studied in detail. One-electron oxidations at around 200 mV vs. ferrocene/ferrocenium were reversible in cyclic voltammograms. UV-vis spectroelectrochemistry reveals spectra characteristic of Ir^{IV} species but also partial decomposition of the oxidised species $[Ir^{IV}Cl_5(RN(H)N=O)]^{\bullet-}$ on this timescale (minutes). Detailed studies on chemically oxidised solutions of the parent Ir^{III} complexes gave evidence for paramagnetic Ir^{IV} from NMR spectra. Final products of the decomposition were the corresponding alcohols and presumably $[Ir^{III}Cl_5(L)]^{2-}$ (L = N_2, solvent, amine) complexes. Similar decomposition reactions of acidic DMSO solutions of $[IrCl_5(RN(H)N=O)]^{2-}$revealed that this combination produces the so-called "activated" DMSO (Me_2S^+-O^- or Me_2S^+-OE, with "E" being an electrophile) which oxidises the parent Ir^{III} complexes. Finally, with the very reactive purple Ir^{IV} compound $(PPh_4)[IrCl_5(BnN(H)N=O)]$, the first primary *N*-nitrosamine coordinated to $[Ir^{IV}Cl_5]^-$ was isolated and characterised by UV-vis absorption, FTIR, NMR spectroscopy, ultra-high resolution electrospray mass spectrometry (UHR-ESI-MS) and iridium L_3 X-ray absorption near-edge spectroscopy (XANES).

1. Introduction

In the last years we could show that the $[Ir^{III}Cl_5(NO)]^-$ scaffold provides an excellent opportunity to react the bound nitrosyl with substrates such as alkenes, thiolates and amines thus forming metal-bound *C*-nitroso compounds,[1] *N*-nitrosothiols,[2,3] and *N*-nitrosamines.[4,5] Several primary N-nitrosamines ($R^1N(H)N=O$) with R^1 = p-toluidine, 2,2,2-trifluoroethylamine, benzylamine, *n*-butylamine, cyclopropylamine, and the pseudoaromatic amine 9-octyladenine have thus been studied (Scheme 1).[6] Primary *N*-nitrosamines are intrinsically unstable but, together with their tautomeric isomers, diazoic acids ($R_1N=N–OH$), they are considered as important intermediates in the deamination of DNA bases[7] and in the formation of diazonium salts,[8,9] which stand for an important area of organic chemistry.[10]

We also found that these $[IrCl_5]^{2-}$ bound primary N-nitrosamines form diazoic acid derivatives which can cleave OH^-, yielding diazonium complexes (Scheme 1).[5,11] When attacked by nucleophiles (Nu) the dioazonium complexes readily cleave ROH and RNu forming N_2 complexes. They can react with amines or solvent to give amino[5] or solvent[11] complexes.

The electrochemistry of the parent complex $[IrCl_5(NO)]^-$ revealing a reversible one-electron reduction at –0.33 V vs ferrocene/ferrocenium in *n*-PrCN at –60°C has been studied quite some time ago together with IR and EPR spectroelectrochemistry and quantum chemical DFT calculations.[12] In contrast to this, the redox chemistry of the *N*-nitrosamine $[IrCl_5]^{2-}$ complexes has

View Article Online
DOI: 10.1039/C8DT02549E

not been investigated. When doing so on a selected couple of complexes $[IrCl_5(RN(H)N=O)]^{2-}$ with R = benzyl ($[\mathbf{1}]^{2-}$) and *n*-butyl ($[\mathbf{2}]^{2-}$), we found reversible oxidation processes indicative for a $Ir^{III/}$ Ir^{IV} couple and chemical follow-up reactions quite similar to the ones described for the reactions with nucleophiles (Scheme 1).

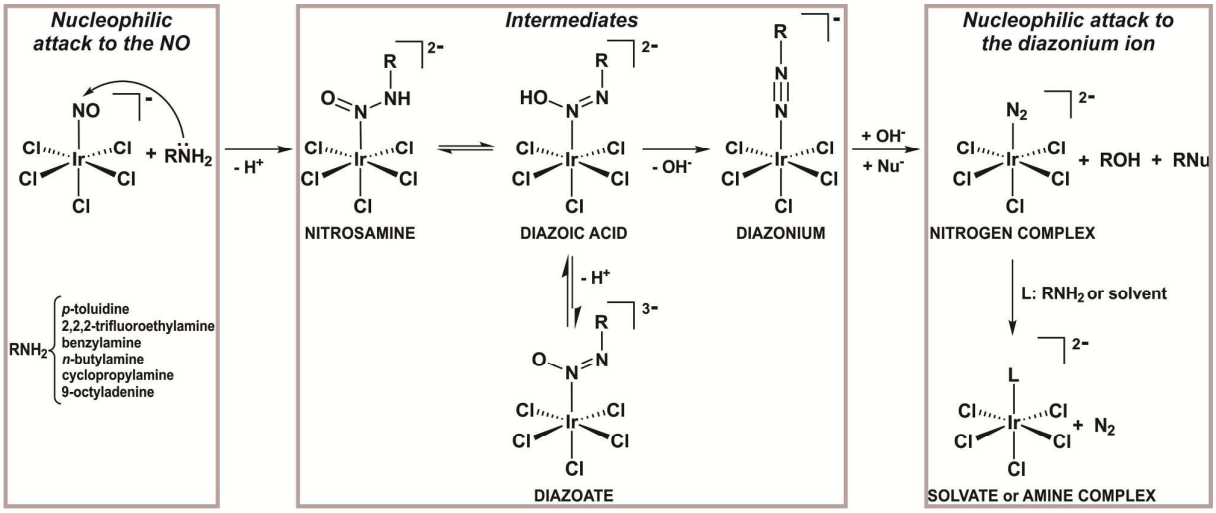

Scheme 1 Formation of *N*-nitrosamine complexes and their reactivity towards nucleophiles. Adopted from ref. 5.

In this contribution we will present results from an in depth study on these oxidation processes using cyclic voltammetry and spectroelectrochemistry applying electrochemical (electrolysis) and chemical oxidation methods. Furthermore, UV-vis absorption, NMR and EPR spectroscopy, ultra-high resolution electrospray mass spectrometry (UHR-ESI-MS) and iridium L_3 X-ray absorption near-edge spectroscopy (XANES) experiments have been carried out on isolated oxidised materials to probe for the oxidation state of the metal centre and the structures of the assumed Ir^{IV} species $[IrCl_5(RN(H)N=O)]^{\bullet-}$.

2. Results and Discussion

2.1 Syntheses and structures of $[Ir^{III}Cl_5(RN(H)N=O)]^{2-}$ complexes (R = benzyl $[1]^{2-}$ or *n*-butyl $[2]^{2-}$)

In order to have a broad arsenal of materials, the parent Ir^{III} complexes $[IrCl_5(RN(H)N=O)]^{2-}$ were synthesised and crystallised together with various cations such as PPh_4^+, K^+, and RNH_3^+ with R = benzyl (Bn) or *n*-butyl (Bu). The isolation of the mixed salts $K(RNH_3)[IrCl_5(RN(H)N=O)]$ is a consequence of syntheses starting from $K[IrCl_5(NO)]$ and RNH_2 (Eq. 1). The PPh_4^+ cations were

View Article Online
DOI: 10.1039/C8DT02549E

introduced for enhanced solubility in organic solvents such as acetonitrile (MeCN) and tetrahydrofurane (THF) for the compounds $(PPh_4)_2[IrCl_5(RN(H)N=O)]$. For details on the synthesis and characterisation, see the Experimental. The molecular structures of $[IrCl_5(BnN(H)N=O)]^{2-}$ and another analogue, $[IrCl_5(TfN(H)N=O)]^{2-}$ (Tf = 2,2,2-trifluoroethyl), as determined by single X-ray diffraction and spectroscopy have been previously reported and seem to be independent of the counter ions.[5]

$$K[IrCl_5(N{\equiv}O)] + 2RNH_2 \xrightarrow{MeCN} K(RNH_3)[IrCl_5(RN(H)N{=}O)]\downarrow \quad (1)$$

2.2 Electrochemical properties of the primary *N*-nitrosamine complexes $[IrCl_5(RN(H)N=O)]^{2-}$

Cyclic voltammetry and UV-vis spectroelectrochemistry of $[\mathbf{1}]^{2-}$ and $[\mathbf{2}]^{2-}$ are shown in Fig. 1 and 2. Both complexes display a one-electron reversible oxidation at $E_{1/2}$ = 311 and 220 mV vs. ferrocene/ferrocenium, for $[\mathbf{1}]^{2-}$ and $[\mathbf{2}]^{2-}$, respectively, which we assign to an oxidation process Ir^{III}/Ir^{IV}. These values are comparable with the Ir^{III}/Ir^{IV} couple observed in hexachloroiridates at 436 mV[13] (value recalculated for DMSO solution from ref. 14) and also are in the range observed in electrochemical studies of other Ir^{III} complexes containing the cyclometalating $^{-}$Phpy (2-phen-2-ide-pyridine) ligands and derivatives (70–910 mV),[15-18] Ir^{III} bis-pyridine-2-sulfonamide complexes (400-550 mV),[19] Ir^{III} corrolates (~200 mV),[20,21] or the complex [Cp*Ir(NHC)Cl] (NHC^{-} = 1-phen-2-ide-3-diphenylimidazol-2-ylidene; Cp* = pentamethylcyclopentadienide; 200 mV).[18] For Ir^{III} pyridine-alkoxide complexes markedly higher values were reported (800–1000 mV).[17,22] The oxidations of $[\mathbf{1}]^{2-}$ and $[\mathbf{2}]^{2-}$ occur reversibly on the timescale of the experiment.

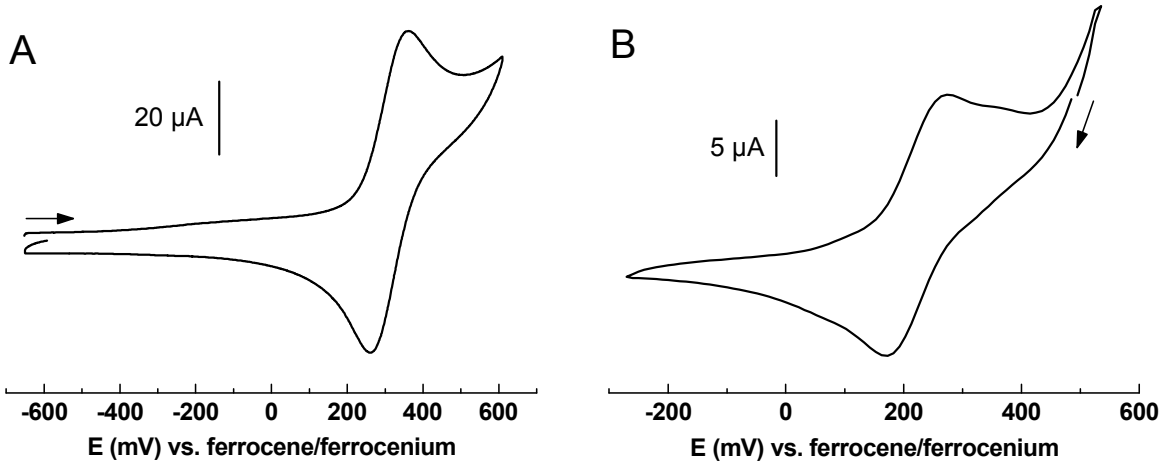

Fig. 1 Cyclic voltammetry of complexes $K(NH_3R)[IrCl_5(RN(H)N=O)]$ in DMSO/nBu$_4$NPF$_6$ at 298 K and at 100 mV/s. **A**: R= benzyl $[\mathbf{1}]^{2-}$; **B**: R= *n*-butyl $[\mathbf{2}]^{2-}$.

The UV-vis spectroelectrochemical anodic oxidation of $[\mathbf{1}]^{2-}$ and $[\mathbf{2}]^{2-}$ (Fig. 2) shows dominating bands of the starting Ir^{III} complexes at about 240 and 335 nm. The bands at 240 nm have large

View Article Online
DOI: 10.1039/C8DT02549E

extinction coefficients and are probably due to ligand-based π–π^* transitions. The rather intense long-wavelength absorptions with maxima at around 335 nm and tailing down to 470 nm can be assigned to ligand-to-metal charge-transfer absorptions (LMCT; RN(H)N=O or Cl^- to Ir^{III}) based on assignments of hexachloroiridates and hydroxyiridates.[23,24,25] Probably they obscure the weak d-d bands occurring also in this spectral range.[24,25]

Upon anodic oxidation, new long-wavelength absorption bands appear at 544 nm for both compounds and the bands at 335 nm are reduced in intensity (Fig. 2). At the same time, the 240 nm (π–π^*) absorptions seem to gain intensity. Isosbestic points are found at 304 and 415 nm for the benzyl complex and at 308 and 432 nm for the butyl derivative. This is in line with a change in the colour of the solution from pale orange to dark purple. The new long-wavelength absorptions at 544 nm are too intense to be considered as d-d transitions (Table S1 in the ESI†). Thus, we assign them to the above mentioned LMCT which is red-shifted upon oxidation in line with a stabilisation of the metal HOMO (highest occupied molecular orbital). This supports our assumption of a metal-based oxidation in the nitrosamine complexes $[Ir^{III/IV}Cl_5(RN(H)N=O)]^{2-/-}$ and the spectral assignment is in line with related Ir^{IV} complexes.[22] Similar strong LMCT (Cl^- to Ir^{IV}) absorptions in this spectral region have been also reported for $[IrCl_6]^{2-}$ [23,24,25] and $[IrCl_5(H_2O)]^-$ [24] in line with our observations.

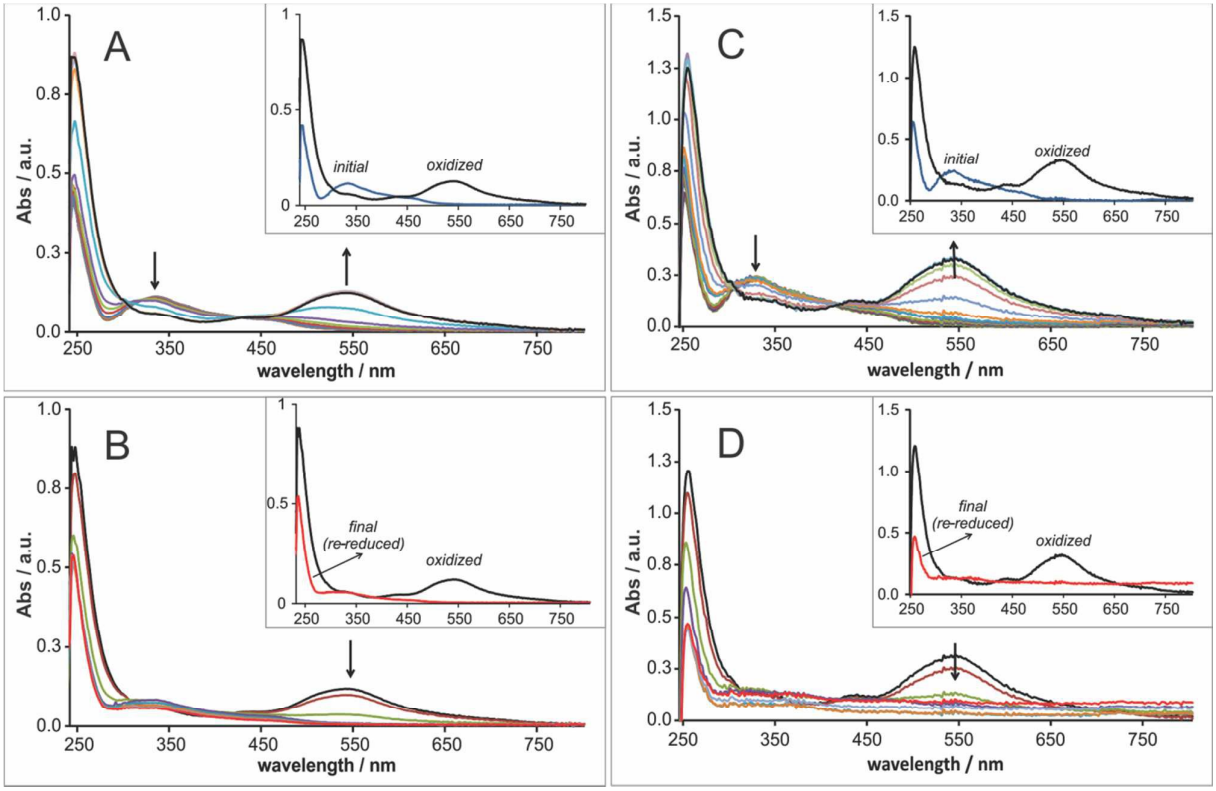

Fig. 2 UV-vis absorption spectra recorded during anodic oxidation of $[\mathbf{1}]^{2-}$ (**A** and **B**) and $[\mathbf{2}]^{2-}$ (**C** and **D**) in DMSO/nBu$_4$NPF$_6$ at room temperature in an OTTLE cell (applied potential 0–800 mV).

View Article Online
DOI: 10.1039/C8DT02549E

Inset **A** and **C**: Parent complex in blue and product of the oxidation in black; inset **B** and **D**: oxidised complex in black and re-reduced complex in red.

At the same time re-reduction after exhaustive oxidation did not completely yield the original spectra (Fig. 2 B and D). Thus, the oxidised species $[Ir^{IV}Cl_5(RN(H)N=O)]^{\bullet-}$ are not stable on the timescale of the UV-vis spectroelectrochemistry experiments which lies in the range of minutes.

2.3 Chemical oxidation of the *N*-nitrosamine complexes $[IrCl_5(RN(H)N=O)]^{2-}$ - in situ spectroscopy

In order to characterise the oxidised complexes $[\mathbf{1}]^{\bullet-}$ and $[\mathbf{2}]^{\bullet-}$ spectroscopically, the oxidation of $[IrCl_5(RN(H)N=O)]^{2-}$ [R = benzyl (Bn) or *n*-butyl (Bu)] was carried out using the chemical oxidants Magic Blue $(N(C_6H_4Br\text{-}4)_3)[SbCl_6]$ (+0.70 V *vs* ferrocene/ferrocenium in CH_2Cl_2)[26,27] and $(NH_4)_2[Ce^{IV}(NO_3)_6]$ (+1.21 V in H_2O).[27,28] The reactions were followed by UV-vis absorption, FTIR, and NMR spectroscopy as well as ultra-high resolution ESI-MS. Although both oxidants seemed to work as was concluded from the observed colour change from orange to purple (R = Bn) or brown-purple (R = Bu), the spectra obtained on reactions using Ce^{IV} were unequivocal, while oxidation using Magic Blue seemed to yield mixtures of species.

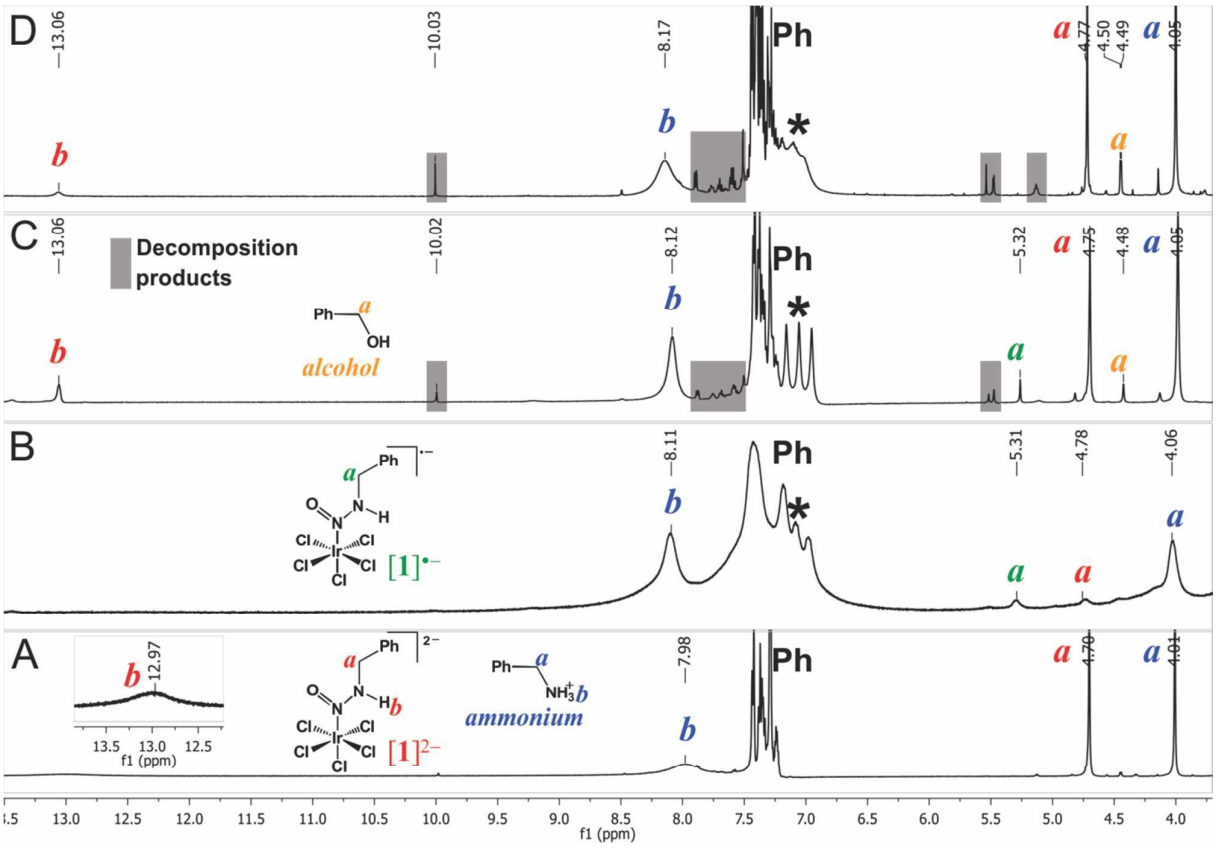

View Article Online
DOI: 10.1039/C8DT02549E

Fig. 3 Oxidation of K(BnNH$_3$)[**1**] in DMSO-d^6 using $(NH_4)_2[Ce(NO_3)_6]$, followed by ^{1}H NMR (500 MHz) spectroscopy. **A**: starting complex. **B:** spectrum recorded immediately after addition. **C**: spectrum recorded after 10 minutes. **D**: spectrum recorded after 3 hours. NH_4^+ protons are indicated with *.

In the NMR spectra of the benzyl derivative K(BnNH$_3$)[**1**] when oxidised with $(NH_4)_2[Ce(NO_3)_6]$ (Fig. 3), three signals in the range 4.5 to 5.5 represent the CH_2 protons of three different benzyl species and we assign them to $[\mathbf{1}]^{2-}$ (4.7 ppm), $[\mathbf{1}]^{\bullet-}$ (5.3 ppm), and benzyl alcohol (4.5 ppm). The CH_2 protons of the $BnNH_3^+$ cation are found at 4.1 ppm. Another interesting aspect is the broadening of the lines after adding the oxidant pointing to a paramagnetic character of the produced complex $[\mathbf{1}]^{\bullet-}$, in line with the assumption of a Ir^{IV} d^5 low-spin configured octahedral species $[IrCl_5(BnN(H)N=O)]^{\bullet-}$. During the reaction, the signals are sharpened again indicative for a back-reduction to Ir^{III}. Very similar observations were made on oxidation of solutions of K(BuNH$_3$)[**2**], $(PPh_4)_2$[**1**] and $(PPh_4)_2$[**2**] in DMSO-d^6 using $(NH_4)_2[Ce^{IV}(NO_3)_6]$ (Fig. S1 to S4 in the ESI†). In many of these experiments we also observed alongside with the alcohols the corresponding aldehydes benzaldehyde and propanal and even benzoic acid and butyric acid.

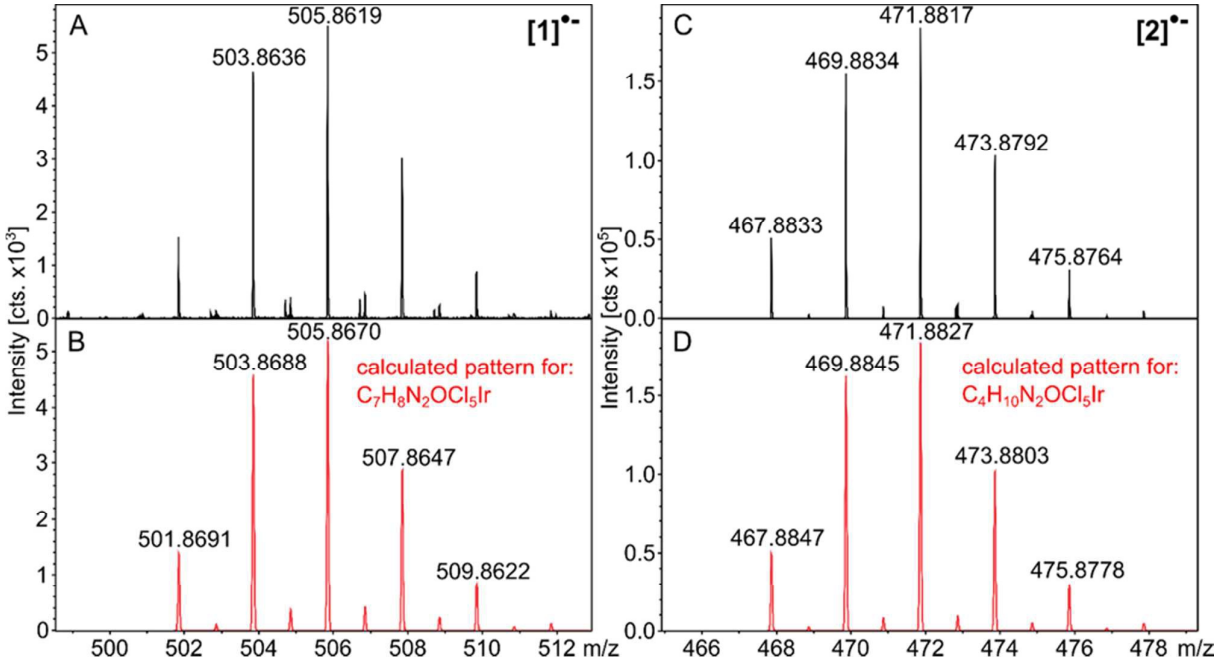

Fig. 4 Ultra-high-resolution electrospray mass spectrometry experiments (UHR-ESI-MS) of the MeOH-solutions oxidised using $(NH_4)_2[Ce^{IV}(NO_3)_6]$ in the negative ion mode (**TOP A+C**, collected data at –60 °C; **Bottom B+D**, simulated isotopic pattern). **Left (A+B)**: results obtained for $[\mathbf{1}]^{\bullet-}$ for the ion $M^{\bullet-} = [Ir^{IV}Cl_5(BnN(H)N=O)]^{\bullet-}$, *m/z* =505.8619 (calc. *m/z* = 505.8670); **Right (C+D)**: results obtained for $[\mathbf{2}]^{\bullet-}$ for the ion $M^{\bullet-} = [Ir^{IV}Cl_5(BuN(H)N=O)]^{\bullet-}$, *m/z* = 471.8817 (calc. *m/z* = 471.8827).

View Article Online
DOI: 10.1039/C8DT02549E

Ultra-high-resolution low-temperature ESI-MS experiments on MeOH-solutions of $(PPh_4)_2$[**1**] and $(PPh_4)_2$[**2**], oxidised *in vitro* with $(NH_4)_2[Ce^{IV}(NO_3)_6]$, at -60 C showed the ions $[Ir^{IV}Cl_5(BnN(H)N=O)]^{\bullet-}$, with a *m/z* = 505.8619 (calc. *m/z* = 505.8670), and $[Ir^{IV}Cl_5(BuN(H)N=O)]^{\bullet-}$, with a *m/z* = 471.8817 (calc. *m/z* = 471.8827), respectively (Fig. 4). Thus, NMR spectroscopy and UHR-ESI-MS gave clear indication for the formation of $[\mathbf{1}]^{\bullet-}$ and $[\mathbf{2}]^{\bullet-}$, the first species in which primary *N*-nitrosamines coordinate to Ir^{IV}. The half-life of the species can be estimated from NMR spectroscopy to about 1 h.

The oxidised solutions were also investigated using X band EPR spectroscopy. Neither solutions at ambient temperature nor at 110 K or 4 K (glassy frozen) gave reasonable signals. We conclude from this that the paramagnetic $[Ir^{IV}Cl_5(RN(H)N=O)]^{\bullet-}$ species are EPR silent due to unfavourable relaxation behaviour. EPR of $[IrCl_6]^{2-}$ has been so far only measured using Ir^{IV} doped lattices, such as $(A)_2[PtCl_6]$ with A = NH_4^+, Na^+ or K^+, while in bulk $K_2[IrCl_6]$ efficient chlorine nuclear relaxation was reported.[29] Thus, we assume the same is happening in $[IrCl_5(RN(H)N=O)]^{\bullet-}$ samples. This is in line with the observation that only extensive hydrolysis of K_2IrCl_6 and thus replacement of all Cl^- ligands allows the observation of a weak EPR signal for such Ir^{IV} species.[23] In contrast to this, broad rhombic or axial EPR spectra of Ir^{IV} have been observed for complexes containing pyridine-alkoxide ligands,[22] for the cationic Ir^{IV} complex $[Cp^*Ir(NHC)Cl]^+$ (NHC^- = 1-phen-2-ide-3-diphenylimidazol-2-ylidene),[18] or for Ir^{IV} corrolates,[20,21] in glassy frozen solutions at temperatures between 4 and 20 K. For the recently reported Ir^{IV}-containing polyoxometalate $[HIr^{IV}W_6O_{24}]^{7-}$ a complex signal was recorded at 110 K from a powder sample.[30]

From all this we can conclude that the oxidised Ir^{IV} complexes $[Ir^{IV}Cl_5(RN(H)N=O)]^{\bullet-}$ undergo decomposition reactions yielding products very much alike those observed previously from decomposition of nitrosamine complexes $[IrCl_5(RN(H)N=O)]^{2-}$ initiated by a loss of OH^- as shown in Scheme 1,[5] which were initially the diazonium complexes and finally amino, N_2 and/or solvent complexes $[Ir^{III}Cl_5(L)]^{2-}$ together with the alcohols ROH. What is different, is the observation of oxidatively produced Ir^{IV} species by NMR and UV-vis and the oxidised products of ROH, aldehydes and carboxylic acids. As one probable mechanism we assume that the Ir^{IV} species $[Ir^{IV}Cl_5(RN(H)N=O)]^{\bullet-}$ cleave the $^{\bullet}OH$ radical and we were able to trap this radical when oxidising $(PPh_4)_2$**[1]** in the presence of the spin trap PBN (*N-tert.*-butyl-α-phenylnitrone) using $(NH_4)_2[Ce(NO_3)_6]$ (Fig. S4†). $^{\bullet}OH$ might also be the oxidant converting the alcohols to aldehydes and carboxylic acids. On the other hand the complexes $[Ir^{IV}Cl_5(RN(H)N=O)]^{\bullet-}$ might also cleave hydroxide OH^- yielding diazonium radical complexes $[Ir^{IV}Cl_5(RNN)]^{\bullet}$ which oxidise organic species and finally decompose to N_2 and solvent complexes $[Ir^{III}Cl_5(L)]^{2-}$.

2.4 Reaction of the nitrosamine complexes $[IrCl_5(RN(H)N=O)]^{2-}$ with acids

View Article Online
DOI: 10.1039/C8DT02549E

The decomposition of $[IrCl_5(RN(H)N=O)]^{2-}$ by acids was studied previously by our group to establish the reactivity patterns shown in Scheme 1.[4-6] When the compounds $K(RNH_3)[IrCl_5(RN(H)N=O)]$ were dissolved in DMSO in the presence of strong acids such as trifluoroacetic acid (TFA), HCl or $HClO_4$, intermediate species could be detected by ^{1}H NMR spectroscopy at 5.3 ppm and 4.3 ppm, identical to those observed for the oxidised benzyl $[\mathbf{1}]^{\bullet-}$ and butyl $[\mathbf{2}]^{\bullet-}$ derivatives, respectively (Fig. 5 and Fig. S5†). The same results were obtained independently of the counter ions K^+ and RNH_3^+ or PPh_4^+ in the DMSO solution (Figs. S6 and S7†). However, for other solvents such as MeCN or MeOH only the previously observed decomposition products (Scheme 1), especially the alcohols, were observed (4.45 and 3.30 ppm for the α H respectively) and not the oxidised complexes (Fig S8†).

From this it is clear that the combination of DMSO and strong acids has acted as oxidant of the nitrosamine complexes $[Ir^{III}Cl_5(RN(H)N=O)]^{2-}$. This is not unexpected since the so-called "activated" DMSO (Me_2S^+-O^- or Me_2S^+-OE, with "E" being an electrophile) has been identified as oxidant in several studies showing that trifluoroacetic acid other acids are activating agents.[31,32]

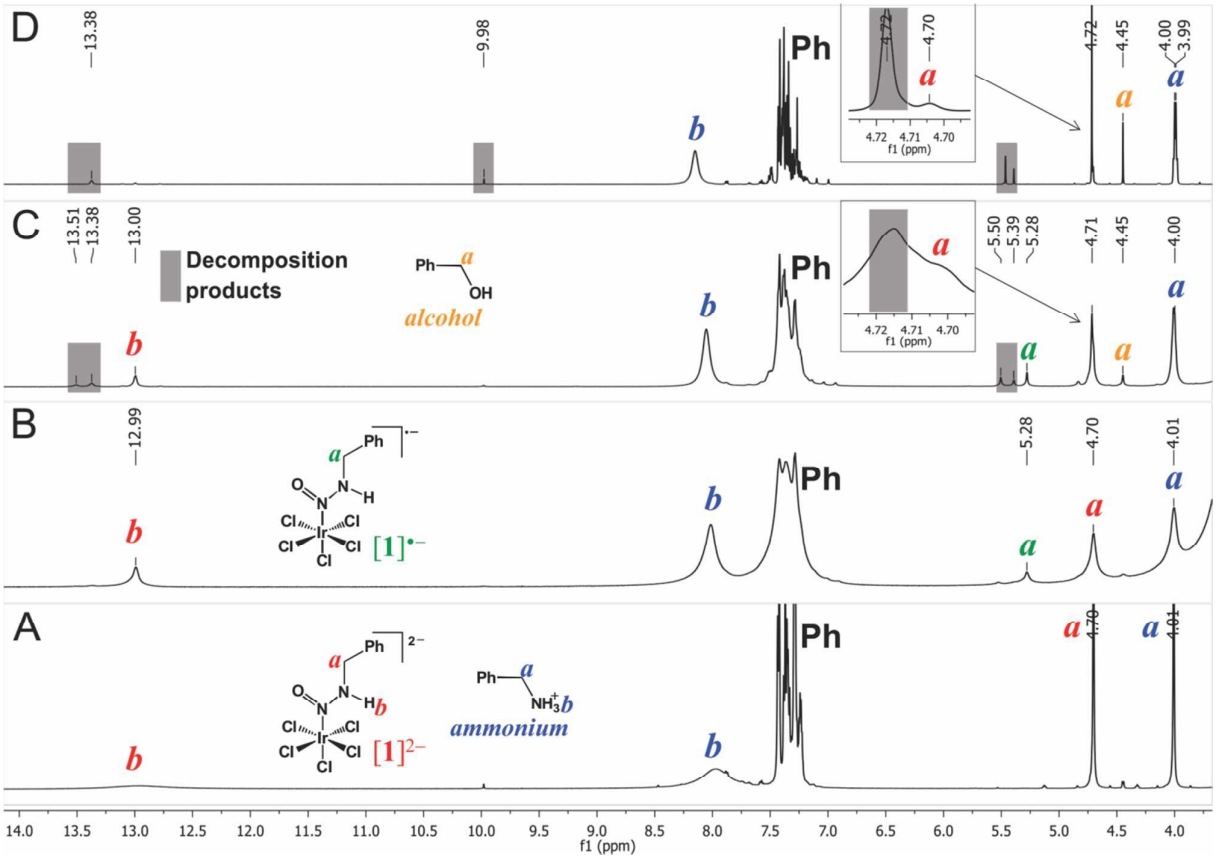

Fig. 5 Decomposition of $K(BnNH_3)[\mathbf{1}]$ in DMSO-d^6/TFA (trifluoroacetic acid) followed by ^{1}H NMR (500 MHz) spectroscopy. **A**: starting complex. **B**: spectrum recorded immediately after addition of 1 equivalent of TFA. **C**: spectrum recorded after 60 min.; **D**: spectrum recorded after 96

View Article Online
DOI: 10.1039/C8DT02549E

h. The intermediate species at 5.28 ppm is assigned to $[\mathbf{1}]^{\bullet-}$, benzyl alcohol is detected at 4.45 ppm, further yet un-identified decomposition products are marked in grey.

2.5 Attempted isolation of the oxidised *N*-nitrosamine complexes $[IrCl_5(RN(H)N=O)]^-$

Stoichiometric reactions of $[IrCl_5(RN(H)N=O)]^{2-}$ (R = benzyl $[\mathbf{1}]^{2-}$ and *n*-butyl $[\mathbf{2}]^{2-}$) with the chemical oxidants Magic Blue and $(NH_4)_2[Ce(NO_3)_6]$ were performed in DMSO, MeOH, MeCN and water at different ratios and temperatures and for different counter ions. The desired product $(PPh_4)[IrCl_5(BnN(H)N=O)]$ could be isolated as a purple material (details in the Experimental) for the reaction of $(PPh_4)_2[IrCl_5(BnN(H)N=O)]$ with $(NH_4)_2[Ce(NO_3)_6]$ in MeOH at –30° C. The UV-vis absorption spectrum of $(PPh_4)[\mathbf{1}]$ dissolved in MeOH showed the characteristic band at ~540 nm (Fig. S9†). UHR-ESI-MS experiments performed on the same solution showed a signal at m/z 505.8656 in agreement with the $[Ir^{IV}Cl_5(BnN(H)N=O)]^{\bullet-}$ ion (calc. m/z = 505.8665). The same procedure applied for $(PPh_4)[\mathbf{2}]$ led to a pale brown solid, probably the solvent-complex based on the ^{1}H NMR and UHR-ESI-MS results and considering the higher instability of $[\mathbf{2}]^{2-}$ and $[\mathbf{2}]^{\bullet-}$ in comparison with $[\mathbf{1}]^{2-}$ and $[\mathbf{1}]^{\bullet-}$.[6,11]

The obtained materials are unstable as can be seen in the rapid decomposition of the Ir^{IV} complex $(PPh_4)[\mathbf{1}]$ (Figs. S10 and S11†). The NMR spectra reveal the same products as observed in the *in situ* measurements, especially large amounts of benzylic alcohol. X band EPR spectroscopy on the isolated material $(PPh_4)[\mathbf{1}]$ gave no signals at 298, 110 and 4 K of the solid materials and for DMSO or THF solutions as observed for the experiments performed in solution described above. Unfavourable relaxation as pointed out above is obviously a problem in our systems.

2.6 XANES measurements

Previously it was shown that in the XANES (X-ray absorption near edge spectroscopy) of the Ir^{III} complex $[IrCl_5(NO)]^-$ at the Ir L_3 edge the absorption energy is identical for the two different counter ions K^+ and PPh_4^+ as expected, but the so-called white-line area is different [33] and it has also been shown that this white-line areas can be correlated to the oxidation state.[33-39]

View Article Online
DOI: 10.1039/C8DT02549E

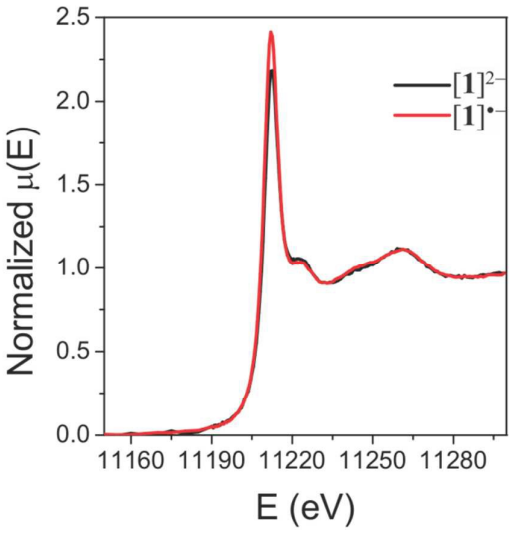

Fig. 6 Normalised XANES spectra at the Ir L_3 edge for the compounds $(PPh_4)_2$[**1**] and (PPh_4)[**1**].

The area of the absorption peak in Fig. 6 at around 11.20 keV for (PPh_4)[**1**] is notably larger than that for $(PPh_4)_2$[**1**], indicating the Ir atom has a higher density of unoccupied states with 5d character in line with the higher oxidation state of $[\mathbf{1}]^{\bullet-}$ compared with $[\mathbf{1}]^{2-}$. The expected energy shift is not observable for the two different samples since the maximum resolution of the measurements of approximately 5 eV is too big for detecting the expected small difference of ca. 1 eV.

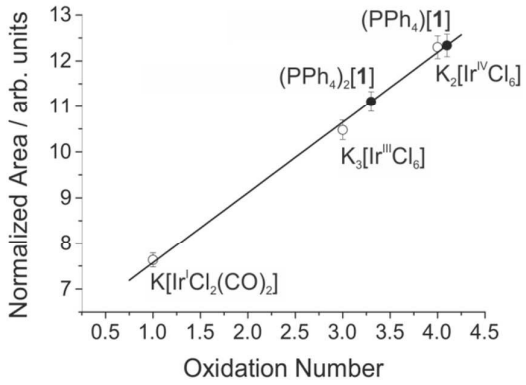

Fig. 7 Correlation of the Ir L_3 white-line area with Ir oxidation states for $(PPh_4)_2$[**1**] and (PPh_4)[**1**]. O: linear fit line for the reference compounds; ●: experimental results for $(PPh_4)_2$[**1**] and (PPh_4)[**1**].

In order to evaluate the oxidation states $(PPh_4)_2$[**1**] and (PPh_4)[**1**] three reference compounds were studied: $K_2[Ir^{IV}Cl_6]$, $K_3[Ir^{III}Cl_6]$ and $K[Ir^{I}Cl_2(CO)_2]$ (Fig. S12†). When plotting the white-line area of all compounds versus their oxidation states (Fig. 7 and S13†) a quite perfect linear relationship is

View Article Online
DOI: 10.1039/C8DT02549E

obtained. Under this approximation, we can derive oxidation states of +3.3 (= III) and +4.1 (= IV), for $(PPh_4)_2$[**1**] and (PPh_4)[**1**], respectively.

3. Experimental

3.1 Instrumentation

^{1}H NMR spectra were recorded using a Bruker AM500 equipped with a broadband probe. ^{1}H shifts are reported relative to DMSO-d^6 (δ = 2.50 ppm). IR spectra were recorded using a Nicolet Avatar 320 FTIR spectrometer with a Spectra Tech cell for KBr pellets. UV-vis absorption spectra were recorded using a Hewlett-Packard 8453 diode array spectrometer in 10 mm optical path quartz cuvettes. GC-mass spectra were recorded on a Shimadzu GC-17A gas chromatograph with a HP Ultra 2 capillary column attached to a GCMS-QP5000 mass spectrometer operating in the positive ion electronic impact ionisation mode at 70 eV. UHR-ESI-MS measurements were performed on a UHR-TOF Bruker Daltonik (Bremen, Germany) maXis plus, an ESI-qTOF-MS capable of resolution of at least 60,000 FWHM. Detection was in negative-ion mode and the source voltage was 3.2 kV. The flow rates were 250 µL per hour. The drying gas (N_2) was held at –55 °C, the spray gas (N_2) was held at –60 °C. The instrument was calibrated prior to every experiment via direct infusion of the Agilent ESI-TOF low concentration tuning mixture, which provided an m/z range of singly charged peaks up to 2700 Da in both ion modes. EPR spectra were recorded in the X band with a Bruker ELEXSYS500E equipped with a Bruker variable-temperature unit ER 4131VT (500 to 100 K) or an Oxford Instruments ESR900 He cryostat (80 to 4 K). The electrochemical measurements of $[IrCl_5(RN(H)N{=}O)]^{2-}$ were performed in DMSO for the K^+ and ammonium salts and in DMSO, MeCN or MeOH for the PPh_4^+ derivatives. Glassy carbon was used as working-electrode and platinum as reference- and counter electrode. nBu$_4$NPF$_6$ was used as the electrolyte in a concentration of 0.1 M and the redox pair ferrocene/ferrocenium was used as reference. Experiments in acidic solutions were also performed using an Ag wire coated with $LiMnO_4$ as reference electrode and Ag as working and counter electrode. $LiBF_4$ was employed as electrolyte. Data were processed using GPES 4.9 (General Electrochemical System Version 4.9). Spectroelectrochemical investigations (UV-vis) were performed at ambient temperature with an OTTLE cell.[40,41] X-ray absorption spectra were measured in a Rigaku R-XAS Looper in-house spectrometer in transmission mode at INIFTA with a Mo target and a Si(400) monochromator crystal. An argon ionisation chamber was used to measure the incident radiation and a solid state detector to measure the transmitted intensity. The energy calibration at the Pt L3 edge (11564 eV) was done using a metallic Pt foil, which is very close to the Ir L3 edge (11215 eV). The XANES

View Article Online
DOI: 10.1039/C8DT02549E

spectra were extracted from the measured absorption spectra by standard methods using the ATHENA software which is part of the IFFEFIT package.[42]

3.2 Materials and procedures.

Unless otherwise noted, all manipulations were performed with exclusion of oxygen and moisture using standard Schlenk procedures and high-vacuum techniques or a MBraun labmaster 130 dry box. Acetonitrile (MeCN) was purchased from J. T. Baker and distilled from CaH_2; diethyl ether was purchased from Cicarelli and distilled from Na-benzophenone; anhydrous DMSO was purchased from Aldrich and used without further purification; anhydrous MeOH was purchased from Merck and purified by distillation. Benzylamine, PPh_4Br, $K_2[IrCl_6]$, $K_3[IrCl_6]$, deuterated solvents and acids were purchased from Sigma-Aldrich and used as received. *n*-butylamine was purchased from Riedel-de Haën and used as received. $K[IrCl_5(NO)]$ was purchased from Strem and purified by recrystallisation from dry MeCN. $K[Ir^{I}Cl_2(CO)_2]$ was synthesised according to ref. 43.

Synthesis of $[IrCl_5(RN(H)N=O)]^{2-}$ (R = Bn or Bu). Nitrosamines $K(NH_3R)$[**1**], $K(NH_3R)$[**2**], $(PPh_4)_2$[**1**] and $(PPh_4)_2$[**2**] were prepared according to ref. 5 and the NMR and MS data agree with those reported there. $(PPh_4)_2[IrCl_5$(*N*-nitrosobutylamine)], $(PPh_4)_2$[**2**], is reported in this work for the first time. Yield: 98%, orange solid. Anal. calcd. for $C_{52}H_{50}Cl_5IrN_2OP_2$ (1150.40): C 54.29; H 4.38; N 2.44; found: C 54.27; H 4.39; N 2.46(%). ^{1}H NMR (DMSO-d^6, ppm): δ = 12.65 (broad s, 0.9H, N<u>H</u>), 8.01–7.92 (m, 8H, Ph_4P^+), 7.88–7.68 (m, 32H, Ph_4P^+), 3.46 (t, 2H, NHC<u>H</u>$_2$), 1.45 (m, 2H, C<u>H</u>$_2$), 1.33 (m, 2H, C<u>H</u>$_2$), 0.85 (t, J = 7.3 Hz, 3H, C<u>H</u>$_3$).

Chemical oxidation of the *N*-nitrosamine complexes $[IrCl_5(RN(H)N=O)]^{2-}$ - in situ spectroscopy

^{1}H NMR, FTIR, UV-vis and UHR-ESI-MS experiments were performed dissolving about 5-10 mg of the starting nitrosamine complexes **[1]**$^{2-}$ (benzyl) or **[2]**$^{2-}$ (*n*-butyl) in DMSO or MeOH (deuterated for NMR) and adding 1 equivalent of Magic Blue $[N(C_6H_4Br\text{-}4)_3][SbCl_6]$, +0.70 V *vs* ferrocene/ferrocenium in CH_2Cl_2)[25,26] or $(NH_4)_2[Ce^{IV}(NO_3)_6]$ (+1.21 V in H_2O).[26,27] In some cases these solutions were quenched with H_2O and then extracted using diethyl ether or $CHCl_3$ for GC-MS experiments. In both cases the corresponding alcohols were the major products alongside with small amounts of the aldehydes and carboxylic esters.

Acid induced decomposition reactions in DMSO solution (oxidation with activated DMSO). ^{1}H NMR experiments were performed dissolving about 5-10 mg of the starting nitrosamine complexes **[1]**$^{2-}$ (benzyl) or **[2]**$^{2-}$ (*n*-butyl) in DMSO-d^6 and adding 1 equivalent of CF_3COOH.

View Article Online
DOI: 10.1039/C8DT02549E

NMR spectra recorded immediately after the reaction with the acid showed a signal at 5.3 ppm and 4.3 ppm for the benzyl and butyl respectively (vs. 4.75 ppm and 3.57 ppm for the corresponding oxidised nitrosamine complexes $[\mathbf{1}]^{\bullet-}$ and $[\mathbf{2}]^{\bullet-}$. The further evolution of the reaction was then followed by ^{1}H NMR spectra recorded at different times. GC-MS experiments were carried out on samples obtained from diethyl ether or $CHCl_3$ extraction of H_2O quenched reaction solutions. In both cases the corresponding alcohols were the major products alongside with small amounts of the aldehydes and carboxylic esters were also identified. The same reaction with other acids like HCl and $HClO_4$ showed similar performance. The same procedure using MeOH-d^4 or MeCN-d^3 as solvents gave to spectral indication for the oxidised nitrosamine complexes $[\mathbf{1}]^{\bullet-}$ and $[\mathbf{2}]^{\bullet-}$ but finally yielded the same decomposition products.

Synthesis of the oxidised complex $(PPh_4)[IrCl_5(BnN(H)N=O)]$. 30 mg of $(PPh_4)_2[\mathbf{1}]$ was dissolved in MeOH (0.7 mL) under an argon atmosphere at –30° (N_2/EtOH slush bath) and then a MeOH solution (0.3 mL) of $(NH_4)_2[Ce(NO_3)_6]$ (30 mg) was added. The reaction solution turned deep purple and a fine purple solid precipitated immediately after the oxidant addition. A few seconds later, a cold solution of ethyl ether:MeOH in a 3:1 ratio was added at low temperature to enhance the precipitation of the solid product. The supernatant was carefully removed and the solid was dried under N_2 current and vacuum. The solid product was characterised by FTIR (pellets). Unfortunately so far, crystallisation only yielded decomposition products or low quality crystalline material. The solid was also dissolved in DMSO or MeOH and characterised by UV-vis, FTIR, NMR, electrochemistry experiments and UHR-ESI-MS showing analogous results to those obtained in the study of the *in situ* oxidation reaction in solution. ^{1}H NMR (DMSO-d^6, ppm): δ = 8.01–7.92 (m, Ph_4P^+), 7.88–7.68 (m, Ph_4P^+), 7.45 (m, Ph), 5.30 (s, $NHC\underline{H}_2Ph$.

Conclusions

The previously studied *N*-nitrosamine complexes $[IrCl_5(RN(H)N=O)]^{2-}$ (R = benzyl $\mathbf{[1]}^{2-}$ or *n*-butyl $\mathbf{[2]}^{2-}$) have been submitted to a detailed study of their redox chemistry. Reversible one-electron oxidations at around 200 mV vs. ferrocene/ferrocenium were observed in cyclic voltammograms on a timescale of a few seconds. UV-vis spectroelectrochemistry reveals bands characteristic of Ir^{IV} species. At the same time, re-reduction after exhaustive oxidation did not completely yield the original spectra and the oxidised species $[Ir^{IV}Cl_5(RN(H)N=O)]^{\bullet-}$ are not stable on the timescale of the UV-vis spectroelectrochemistry experiments which lies in the range of minutes. For a deeper insight, solutions of the parent Ir^{III} complexes were oxidised chemically using Magic Blue or

View Article Online
DOI: 10.1039/C8DT02549E

$(NH_4)_2[Ce(NO_3)_6]$ and *in situ* NMR and EPR spectroscopy and UHR-ESI-MS was carried out. The oxidation from the diamagnetic Ir^{III} starting materials to paramagnetic Ir^{IV} could be monitored through line broadening of NMR spectra but failed to give EPR spectra. In the course of the following decomposition reactions (half-life ~1 h), the NMR spectra regained the initial high resolution and narrow lines indicating a back-reduction to Ir^{III} in line with UV-vis absorption spectra. Furthermore, the corresponding alcohols benzyl and butyl alcohol together with smaller amounts of the aldehydes and carboxylic acids were detected by NMR and MS. Remarkably, the acid-induced decomposition of nitrosamine complexes $[IrCl_5(RN(H)N=O)]^{2-}$ initiated by a loss of OH^- as shown in Scheme 1 yields very similar final products. The oxidatively produced Ir^{IV} species decompose yielding first diazonium complexes and finally amino, N_2 or solvent complexes $[IrCl_5(L)]^{2-}$ together with the ROH. The only difference is the appearance of oxidised complexes $[\mathbf{1}]^{\bullet-}$ and $[\mathbf{2}]^{\bullet-}$and the oxidised products of ROH, the aldehydes and carboxylic acids. As a consequence, we also followed decomposition reactions of the complexes $[IrCl_5(RN(H)N=O)]^{2-}$ through acids by NMR spectroscopy and found that DMSO solutions of the species in the presence of strong acids such as trifluoroacetic acid (TFA), HCl or $HClO_4$ showed very similar decomposition products this time including strong evidence for the intermediate Ir^{IV} species. It became clear that the combination of DMSO and acid produces the so-called "activated" DMSO (Me_2S^+-O^- or Me_2S^+-OE, with "E" being an electrophile) which is able to oxidise the parent Ir^{III} complexes.

As one probable mechanism for the oxidatively-induced decomposition we assume that the Ir^{IV} species $[Ir^{IV}Cl_5(RN(H)N=O)]^{\bullet-}$ cleave the $^{\bullet}OH$ radical and were able to trap this when oxidising $(PPh_4)_2$**[1]** in the presence of the spin trap PBN (*N-tert.*-butyl-α-phenylnitrone) using $(NH_4)_2[Ce(NO_3)_6]$.

Finally, chemical oxidation using $(NH_4)_2[Ce(NO_3)_6]$ at low temperatures allowed to prepare the very reactive Ir^{IV} compound $(PPh_4)[IrCl_5(BnN(H)N=O)]$ as a purple material, representing the first primary *N*-nitrosamines coordinated to $[Ir^{IV}Cl_5]^-$. Further trials especially on the butyl derivative failed. The compound was characterised by UV-vis absorption, FTIR, NMR spectroscopy, UHR-ESI-MS and Ir EXAFS. UV-vis absorption, FTIR, NMR, and MS spectra are fully in line with the results from our *in situ* experiments. Again no EPR signals were observed which we ascribe to unfavourable relaxation. Using Ir^{III} and Ir^{IV} reference compounds, correlation of the Ir L_3 white-line area of XANES spectra with Ir oxidation states allowed an assignment of oxidation states of the Ir metal centre of III and IV for $(PPh_4)_2$[**1**] and (PPh_4)[**1**], respectively.

Conflicts of interest

There are no conflicts to declare.

View Article Online
DOI: 10.1039/C8DT02549E

Acknowledgements

This work was financially supported by Deutscher Akademischer Austauschdienst–Ministerio Nacional de Ciencia y Tecnologia (DAAD-MINCyT) (grant number 50752227), by the Deutsche Forschungsgemeinschaft (DFG)–Consejo Nacional de Investigaciones Cientificas y Tecnicas (CONICET) (COOPINT DFG-CONICET) (grant to A. K.); the DFG projects KL1194/12-1 and KL1194/13-1; PICT 2014-1278 and UBACYT 20020130100642BA (grants to F. D.); PICT 2012-1335 (grant to F. D. S.). and Universidad Nacional de La Plata (UNLP). A. F. acknowledges the Universidad de Buenos Aires (UBA) and CONICET for her scholarships. We thank Dr. Damián Bikiel for providing the complex $K[Ir^{I}Cl_2(CO)_2]$.

References

1 N. Escola, A. Llebaría, G. Leitus and F. Doctorovich, Formation of Coordinated *C*-Nitroso Compounds by Reaction of $K[IrCl_5NO]$ with Alkenes, *Organometallics*, 2006, **25**, 3799–3801.

2 L. L. Perissinotti, D. A. Estrin, G. Leitus and F. Doctorovich, A Surprisingly Stable S-Nitrosothiol Complex, *J. Am. Chem. Soc*., 2006, **128**, 2512–2513.

3 L. L. Perissinotti, D. A. Estrin, G. Leitus, L. Shimon and F. Doctorovich, A Unique Family of Stable and Water-Soluble *S*-Nitrosothiol Complexes, *Inorg. Chem*., 2008, **47**, 4723-4733.

4 F. Doctorovich, F. Di Salvo, N. Escola, C. Trápani and L. Shimon, Formation of Coordinated Nitrosamines by Reaction of $K[IrCl_5NO]$ with Primary Amines, *Organometallics*, 2005, **24**, 4707−4709.

5 F. Di Salvo, D. A. Estrin, G. Leitus and F. Doctorovich, Synthesis, Structure, and Reactivity of Aliphatic Primary Nitrosamines Stabilized by Coordination to $[IrCl_5]^{2-}$, *Organometallics*, 2008, **27***,* 1985–1995.

6 F. Doctorovich, F. Di Salvo, Performing Organic Chemistry with Inorganic Compounds: Electrophilic Reactivity of Selected Nitrosyl Complexes, *Acc. Chem. Res*., 2007, **40**, 985−993.

7 J. Caulfield, J. Wishnok and S. Tannenbaum, Nitric Oxide-induced Deamination of Cytosine and Guanine in Deoxynucleosides and Oligonucleotides, *J. Biol. Chem*., 1998, **273**, 12689−12695.

8 J. R. Mohrig and K. Keegstra, Alkyldiazonium Cations. I. Direct Observation of the 2,2,2-Trifluoroethyldiazonium Ion, *J. Am. Chem. Soc*., 1967, **89**, 5492−5493.

9 D. Berner and J. F. McGarrity, Direct Observation of the Methyl Diazonium Ion in Fluorosulfuric Acid, *J. Am. Chem. Soc*., 1979, **101**, 3135−3136.

View Article Online
DOI: 10.1039/C8DT02549E

10 F. Mo, G. Dong, Y. Zhang and J. Wang, Recent Applications of Arene Diazonium Salts in Organic Synthesis, *Org. Biomol. Chem.*, 2013, **11**, 1582−1593.

11 B. M. Ridgway, A. Foi, R. S. Corrêa, D. E. Bikiel, J. Ellena, F. Doctorovich and F. Di Salvo, Conformational and structural diversity of iridium dimethyl sulfoxide complexes, *Acta Crystallogr., Sect. B: Struct. Sci.,* 2017, **73**, 1032–1042.

12 M. Sieger, B. Sarkar, S. Záliš, J. Fiedler, N. Escola, F. Doctorovich, J. A. Olabe and W. Kaim, Establishing the NO Oxidation State In Complexes $[Cl_5(NO)M]^{n-}$, M = Ru or Ir, through Experiments and DFT Calculations, *Dalton Trans*., 2004, 1797–1800.

13 P. George, I. H. Hanania and D. H. Irvine, A Potentiometric Study of the Chloroiridate-Chloroiridite Couple, *J. Chem. Soc*., 1957, 3048−3052.

14 J. P. Chang, E. Y. Fung and J. C. Curtis, Evidence for Specific Solvent-Solute Interactions as a Major Contributor to the Franck-Condon Energy in Intervalence-Transfer Absorptions of Ruthenium Ammine Complexes, *Inorg. Chem.,* 1986, **25**, 4233–4241.

15 A. B. Tamayo, B. D. Alleyne, P. I. Djurovich, S. Lamansky, I. Tsyba, N. N. Ho, R. Bau and M. E. Thompson, Synthesis and Characterization of Facial and Meridional Tris-cyclometalated Iridium(III) Complexes, *J. Am. Chem. Soc*., 2003, **125**, 7377–7387.

16 S. Jung, Y. Kang, H.S. Kim, Y.-H. Kim, C.-L. Lee, J.-J. Kim, S.-K. Lee and S.-K. Kwon, Effect of Substitution of Methyl Groups on the Luminescence Performance of Ir^{III} Complexes: Preparation, Structures, Electrochemistry, Photophysical Properties and Their Applications in Organic Light-Emitting Diodes (OLEDs), *Eur. J. Inorg. Chem*., 2004, 3415–3423.

17 D. Y. Shopov, B. Rudshteyn, J. Campos, V. S. Batista, R. H. Crabtree and G. W. Brudvig, Stable Iridium(IV) Complexes of an Oxidation-Resistant Pyridine-Alkoxide Ligand: Highly Divergent Redox Properties Depending on the Isomeric Form Adopted, *J. Am. Chem. Soc*., 2015, **137**, 7243–7250.

18 T. P. Brewster, J. D. Blakemore, N. D. Schley, C. D. Incarvito, N. Hazari, G. W. Brudvig and R. H. Crabtree, An Iridium(IV) Species, $[Cp^*Ir(NHC)Cl]^+$, Related to a Water-Oxidation Catalyst, *Organometallics*, 2011, **30**, 965–973.

19 M. Li, K. Takada, J. I. Goldsmith and S. Bernhard, Iridium(III) Bis-Pyridine-2-Sulfonamide Complexes as Efficient and Durable Catalysts for Homogeneous Water Oxidation, *Inorg. Chem*., 2016, **55**, 518–526.

20 J. H. Palmer, A. Mahammed, K. M. Lancaster, Z. Gross and H. B. Gray, Structures and Reactivity Patterns of Group 9 Metallocorroles, *Inorg. Chem*., 2009, **48**, 9308–9315.

21 S. S. Dong, R. J. Nielsen, J. H. Palmer, H. B. Gray, Z. Gross, S. Dasgupta and W. A Goddard, Electronic Structures of Group 9 Metallocorroles with Axial Ammines, *Inorg. Chem*., 2011, **50**, 764–770.

View Article Online
DOI: 10.1039/C8DT02549E

22 D. Y. Shopov, B. Rudshteyn, J. Campos, D. J. Vinyard, V. S. Batista, G. W. Brudvig and R. H. Crabtree, A full set of iridium(IV) pyridine-alkoxide stereoisomers: highly geometry-dependent redox properties, *Chem. Sci*., 2017, **8**, 1642–1652.

23 Y. Zhao, N. M. Vargas-Barbosa, M. E. Strayer, N. S. McCool, M.-E. Pandelia, T. P. Saunders, J. R. Swierk, J. F. Callejas, L. Jensen and T. E. Mallouk, Understanding the Effect of Monomeric Iridium(III/IV) Aquo Complexes on the Photoelectrochemistry of $IrO_x \cdot nH_2O$-Catalyzed Water-Splitting Systems, *J. Am. Chem. Soc.,* 2015, **137**, 8749–8757.

24 L. Moggi, G. Varani, M. F. Manfrin, V. Balzani, Photochemical reactions of hexachloroiridate(IV) Ion, *Inorg. Chim. Acta*, 1970, **4**, 335–341.

25 C. K. Jorgensen, Electron Transfer Spectra of Hexahalide Complexes, *Mol. Phys*., 1959, **2**, 309–332.

26 M. Quiroz-Guzman and S. N. Brown, Tris(4-bromophenyl)aminium hexa-chloridoantimonate ('Magic Blue'): a strong oxidant with low inner-sphere reorganization, *Acta Crystallogr. Sect. C, Cryst. Struct. Commun.*, 2010, **C66**, m171–m173.

27 N. G. Connelly and W. E. Geiger, Chemical Redox Agents for Organometallic Chemistry, *Chem. Rev.,* 1996, **96**, 877–910.

28 G. F. Smith and C. A. Getz, Cerate Oxidimetry, *Ind. Eng. Chem., Anal. Ed.*, 1938, **10**, 191–195.

29 K. R. Jeffrey, R. L. Armstrong and K. E. Kisman, Chlorine Nuclear Relaxation in Paramagnetic K_2IrCl_6, *Phys. Rev. B*., 1970, **1**, 3770–3776.

30 S. A. Adonin, N. V. Izarova, C. Besson, P. A. Abramov, B. Santiago-Schübel, P. Kögerler, V. P. Fedin and M. N. Sokolov, An Ir^{IV}-containing polyoxometalate, *Chem. Commun.*, 2015, **51**, 1222–1225.

31 C. Li, Y. Xu, M. Lu, Z. Zhao, L. Liu, Z. Zhao, Y. Cui, P. Zheng, X. Ji and G. Gao, A Novel and Efficient Oxidation of Benzyl Alcohols to Benzaldehydes with DMSO Catalyzed by Acids, *Synlett,* 2002, 2041–2042.

32 W. W. Epstein and W. Sweat, Dimethyl Sulfoxide Oxidations, *Chem. Rev.,* 1967**, 67**, 247−260.

33 F. Di Salvo, N. Escola, D. A. Scherlis, D. A. Estrin, C. Bondía, D. Murgida, J. M. Ramallo–López, F. G. Requejo, L. Shimon and F. Doctorovich, Electronic Perturbation in a Molecular Nanowire of $[IrCl_5(NO)]^-$ Units, *Chem.-Eur. J.* 2007, **13**, 8428–8436.

34 M. T. Vagnini, M. W. Mara, M. R. Harpham, J. Huang, M. L. Shelby, L. X. Chenab and M. R. Wasielewski, Interrogating the photogenerated Ir(IV) state of a water oxidation catalyst using ultrafast optical and X-ray absorption spectroscopy, *Chem. Sci.*, 2013, **4**, 3863–3873.

35 A. Minguzzi, O. Lugaresi, E. Achilli, C. Locatelli, A. Vertova, P. Ghigna and S. Rondinini, Observing the Oxidation State Turnover in Heterogeneous Iridium-Based Water Oxidation Catalysts, *Chem. Sci.,* 2014, **5**, 3591–3597.

View Article Online
DOI: 10.1039/C8DT02549E

36 J. M. Ramallo-López, E. J. Lede, F. G. Requejo, J. A. Rodriguez, J.-Y. Kim, R. Rosas-Salas and J. M. Dominguez, XANES Characterization of Extremely Nanosized Metal-Carbonyl Subspecies (Me = Cr, Mn, Fe, and Co) Confined into the Mesopores of MCM-41 Materials, *J. Phys. Chem. B.,* 2004, **108**, 20005–20010.

37 T. Pauporte, D. Aberdam, J.-L. Hazemann, R. Faure and R. Durand, X-ray absorption in relation to valency of iridium in sputtered iridium oxide films, *J. Electroanal. Chem.*, 1999, **465**, 88–95.

38 J.-H. Choy, D.-K. Kim, S.-H. Hwang, G. Demazeau and D.-Y. Jung, XANES and EXAFS Studies on the Ir-O Bond Covalency in Ionic Iridium Perovskites, *J. Am. Chem. Soc*., 1995, **117**, 8557–8566.

39 J.-H. Choy, D.-K. Kim, G. Demazeau, D.-Y. Jung, L_{III}-Edge XANES Study on Unusually High Valent Iridium in a Perovskite Lattice, *J. Phys. Chem.*, 1994, **98**, 6258–6262.

40 W. Kaim and J. Fiedler, Spectroelectrochemistry: the Best of two Worlds, *Chem. Soc. Rev.,* 2009, **38**, 3373–3382.

41 M. Krejčik, M. Daněk and F. Hartl, Simple Construction of an Infrared Optically Transparent Thin-Layer Electrochemical Cell. Applications to the Redox Reactions of Ferrocene, $Mn(CO)_3$(3,5-di-t-butyl-catecholate)$^-$, *J. Electroanal. Chem.*, 1991, **317**, 179–187.

42 B. Ravel and M. Newville, ATHENA, ARTEMIS, HEPHAESTUS: Data Analysis for X-ray Absorption Spectroscopy Using IFEFFIT, *J. Synchrotron Rad.*, 2005, **12**, 537–541.

43 D. E. Bikiel, J. M. Ramallo-López, F. G. Requejo, O. B. Oña, M. B. Ferraro, J. C. Facelli and F. Doctorovich, Formation of one dimensional linear chains by Ir–Ir bonds in *cis*-dicarbonyldichloroiridate(I), *Polyhedron*, 2011, **30**, 221–227.

View Article Online
DOI: 10.1039/C8DT02549E

For Table of Contents only

Short text

The one electron oxidation of the *N*-nitrosamine complexes $[Ir^{III}Cl_5(RN(H)N=O)]^{2-}$ (R = benzyl or *n*-butyl) was studied in detail and the reactive purple Ir^{IV} compound $(PPh_4)[IrCl_5(BnN(H)N=O)]$ was isolated.

Pictorial